https://scilett-fsg.uitm.edu.my/
Vol. 17(1) JANUARY 2023

ISSN: 1675-7785
eISSN: 2682-8626

DOI: 10.24191/sl.v17i1.18897

Impact of Annealing Towards Anti-Reflection Properties of Al_2O_3 on Silicon

Halo Dalshad Omar[1,2], Md. Roslan Hashim[1] and Mohd Zamir Pakhuruddin[1,3,*]

[1]*Photovoltaic Materials and Devices, School of Physics, Universiti Sains Malaysia, 11800 Minden, Penang, Malaysia.*

[2]*Department of Physics, Faculty of Science and Health, Koya University, Koya KOY45, Kurdistan Region - F.R. Iraq.*

[3]*Institute of Nano Optoelectronics Research and Technology (INOR), Universiti Sains Malaysia, 11800 USM, Penang, Malaysia.*

Corresponding author: *zamir@usm.my*

Accepted: 9 December 2022; Published: 21 January 2023

ABSTRACT

This paper investigates the impact of annealing towards the anti-reflection properties of aluminium oxide (Al_2O_3) on planar monocrystalline silicon (mono c-Si) wafers. Al_2O_3 anti-reflection coating (ARC) with 120 nm thickness is deposited on the c-Si wafers by radio frequency (RF) sputtering process at room temperature, with the power of 200 Watt and at a base pressure of 5×10^{-5} mbar. This is followed by annealing at different temperatures (700-900 ^{o}C) for 20 min. The results show that the root means square (RMS) surface roughness of the Al_2O_3 increases with increased annealing temperature. The Al_2O_3 films with annealing illustrate lower broadband reflection than the Al_2O_3 without annealing within the 300-1100 nm wavelength region. The Al_2O_3 film annealed at 900 ^{o}C exhibits the lowest reflection (6%) and the highest absorption (94%) at a wavelength of 600 nm with an average weighted reflection (AWR) of 20.4%, owing to the high RMS roughness and the effect of the intermediate refractive index of the Al_2O_3 layer. This results in a maximum potential short-circuit current density ($J_{sc(max)}$) of 37.3 mA/cm^2, which corresponds to a 5.4% enhancement compared to the Al_2O_3 on planar c-Si without an annealing process.

Keywords: *Annealing; antireflection; Al_2O_3; silicon*

https://scilett-fsg.uitm.edu.my/
Vol. 17(1) JANUARY 2023

ISSN: 1675-7785
eISSN: 2682-8626

DOI: 10.24191/sl.v17i1.18897

INTRODUCTION

Crystalline silicon (c-Si) solar cells dominate over 90% of the worldwide photovoltaic (PV) market share due to improving conversion efficiency, reducing technology cost, technology maturity and proven stability [1, 2]. Since the c-Si in its original form exhibits high reflection (around 35-40% in the visible region) and poor light absorption, effective light management strategies are inevitable in the c-Si solar cells [3, 4]. In industrial monocrystalline (mono c-Si) solar cells, this is mitigated by incorporating microscale front pyramids on the c-Si surface, which scatter the incident light into oblique angles, resulting in lower broadband reflection and improved light absorption within 300-1100 nm wavelength region [5, 6]. Apart from that, a silicon nitride (Si_3N_4) anti-reflection coating (ARC) is deposited on the pyramids to further suppress the broadband reflection to below 3%, particularly near the wavelength of 600 nm, which represents the peak of AM1.5G solar spectrum [7, 8]. The reflection suppression is possible because the SiN_x ARC has an optimum intermediate refractive index (n=2.0) to enable the quarter-wavelength AR effect [9, 10]. The suppressed reflection improves light-coupling into the c-Si, leading to increased broadband light absorption by the solar cells.

In the literature, various materials have been evaluated as ARC on c-Si solar cells, such as Si_3N_4, silicon dioxide (SiO_2) and aluminium oxide (Al_2O_3) [11, 12]. Al_2O_3 is a promising dielectric material with high transparency and refractive index n of 1.6 at a wavelength of 600 nm [13, 14]. Various techniques have been reported in the literature to deposit Al_2O_3, such as pulsed laser deposition, sputtering and atomic layer deposition (ALD) [14]. Recently, the fabrication of $Al_2O_3/Si/Al_2O_3$ by ALD (with 23 nm thickness) at different temperatures from 300 ^oC to 750 ^oC has been studied by Zhao et al. [15]. In another study by Singh et al. [13], Al_2O_3 ARC is deposited on p-type c-Si wafers by radio frequency (RF) sputtering, followed by annealing. As a result, the refractive index of the Al_2O_3 increases from 1.70 to 1.75 with increasing annealing temperature (350 to 600 ^oC), and the local rearrangement of the atoms Al_2O_3 after annealing increases the coat density [13].

In this work, the impact of annealing towards the anti-reflection properties of Al_2O_3 ARC on c-Si is investigated. The Al_2O_3 ARC layers are deposited on planar c-Si wafers by RF sputtering. Then, the layers are subjected to different annealing temperatures. Surface morphological and optical properties of the Al_2O_3 layers are then characterised. The relationship between average weighted reflection (AWR) and different annealing temperatures is analysed. From the absorption curve, potential short-circuit current density ($J_{sc(max)}$) is used to estimate the light-coupling performance of the Al_2O_3 ARC layers within the 300-1100 nm wavelength region. From the possible results, $J_{sc(max)}$ enhancement is calculated for each sample. The results demonstrate the importance of the annealing process in reducing the broadband reflection and improving the potential $J_{sc(max)}$ that will be useful in c-Si solar cells.

https://scilett-fsg.uitm.edu.my/
Vol. 17(1) JANUARY 2023

ISSN: 1675-7785
eISSN: 2682-8626

DOI: 10.24191/sl.v17i1.18897

EXPERIMENTAL

N-type (100) mono c-Si wafers with a thickness of 280 µm and resistivity of 5-10 Ω.cm are used in this experiment. Figure 1 illustrates the flow chart of the methodology used in this work. The c-Si wafers are cleaned by the Radio Corporation of America (RCA) technique to eliminate impurities such as organic residuals, metal contaminants and native oxide layer on the wafer surface [16]. After the RCA process, Al_2O_3 ARC with 120 nm thickness is deposited on the planar mono c-Si wafers by RF sputtering at room temperature, using RF power of 200 Watt and base pressure of 5×10^{-5} mbar. The schematic of the Al_2O_3 ARC on the c-Si wafer is illustrated in Figure 2. After the sputtering process, the Al_2O_3 layer on planar c-Si wafers is annealed at different temperatures (700 °C, 800 °C and 900 °C) for 20 min in nitrogen (N_2) gas with a flow rate of 2 L/min.

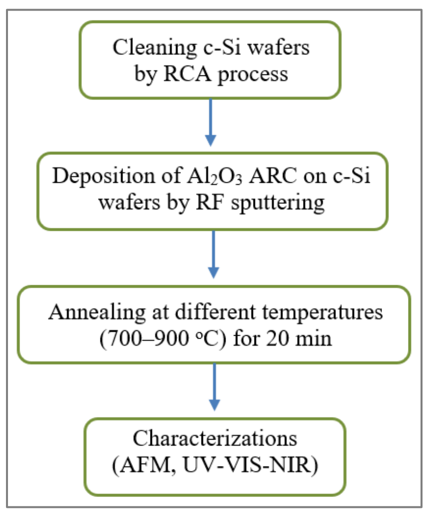

Figure 1: Flow chart of the methodology used in this work.

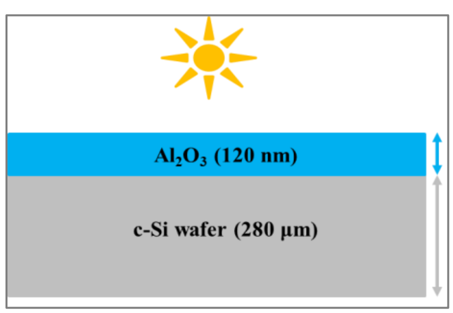

Figure 2: Schematic of Al_2O_3 ARC on the c-Si wafer. Note that the diagram is not to scale.

https://scilett-fsg.uitm.edu.my/
Vol. 17(1) JANUARY 2023
ISSN: 1675-7785
eISSN: 2682-8626

DOI: 10.24191/sl.v17i1.18897

For characterisations of the Al_2O_3 ARC surface morphological properties on c-Si wafers, atomic force microscopy (AFM) is used (model: Bruker Dimension Edge). AFM scan area of 10 μm × 10 μm and resolution of 512 data points are used to determine root means square (RMS) surface roughness. Optical properties of the Al_2O_3 are investigated by measuring the reflection (R) and transmission (T) using Agilent technologies Cary 5000 UV-Vis-NIR spectrophotometer (with integrating sphere). From the reflection profile, average weighted reflection (AWR) is calculated throughout the entire spectral region (300-1100 nm) using Equation (1) [17].

$$\mathrm{AWR}(\lambda) = \frac{\int_{\lambda=300nm}^{\lambda=1100nm} R(\lambda)S(\lambda)d\lambda}{\int_{\lambda=300nm}^{\lambda=1100nm} S(\lambda)d\lambda} \qquad (1)$$

The reflection profile is then used to calculate absorption, using the relation: A = (100–R–T) % [18]. Transmission is equal to zero since the c-Si wafers are opaque. From the absorption result, the light-coupling performance of the Al_2O_3 ARC on c-Si is assessed using a concept of potential $J_{sc(max)}$. The potential $J_{sc(max)}$ is calculated by using Equation (2) for the 300-1100 nm wavelength region [19].

$$J_{sc(max)} = q\int_{\lambda=300nm}^{\lambda=1100nm} \mathrm{EQE}(\lambda).S(\lambda)d\lambda \qquad (2)$$

where q represents the electron charge, λ is the wavelength of light, EQE is the external quantum efficiency (EQE=IQE×A), IQE is internal quantum efficiency (in this calculation, IQE=1), and S(λ) is the standard spectral photon density of AM1.5G solar spectrum.

RESULTS AND DISCUSSION

Surface morphological properties

Figure 3 (a)-(d) depicts AFM images of the Al_2O_3 on planar c-Si without annealing (i.e. as-deposited) and with different annealing temperatures (700-900 ^oC). From the AFM images, it can be observed that the surface roughness of the Al_2O_3 surface increases with the increasing annealing temperature. The RMS roughness of 1.9 nm is obtained for the as-deposited layer. With annealing, the RMS roughness increases with increasing annealing temperature; 4.4 nm, 7.3 nm and 10.7 nm for annealing temperatures of 700 ^oC, 800 ^oC and 900 ^oC, respectively. The increased RMS roughness corroborates well with the findings of Wang et al. [20] after annealing Al_2O_3 films deposited on c-Si wafers (using ALD) with temperatures of 400-900 ^oC.

https://scilett-fsg.uitm.edu.my/
Vol. 17(1) JANUARY 2023

ISSN: 1675-7785
eISSN: 2682-8626

DOI: 10.24191/sl.v17i1.18897

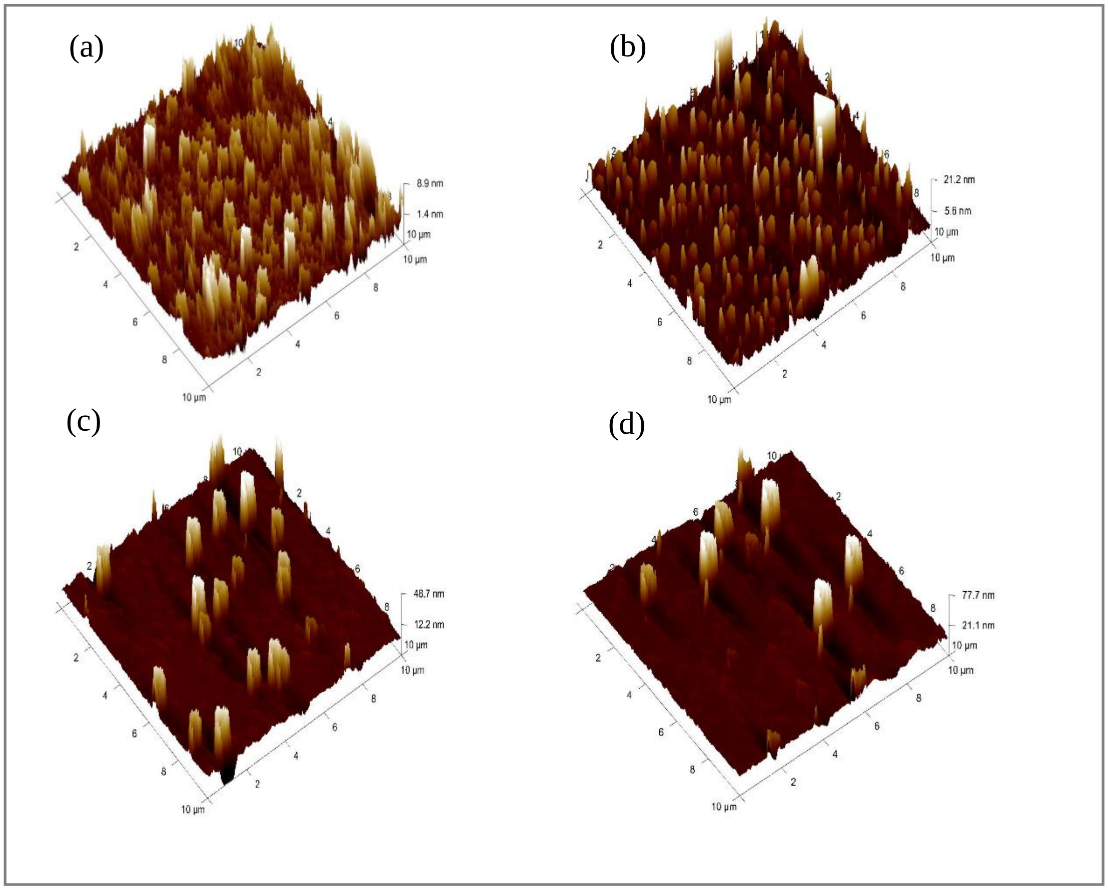

Figure 3: AFM images of Al_2O_3 on planar c-Si for (a) as-deposited (RMS roughness = 1.9 nm) and with annealing temperature of (b) 700 ºC (RMS roughness = 4.4 nm), (c) 800 ºC (RMS roughness = 7.3 nm) and (d) 900 ºC (RMS roughness = 10.7 nm).

Optical properties

Figures 4 (a) and (b) illustrate total reflection and absorption curves for Al_2O_3 ARC on planar c-Si wafers without annealing (as-deposited) and with different annealing temperatures within 300-1100 nm region. The total reflection and absorption curves for Al_2O_3 on planar c-Si without annealing are compared. The Al_2O_3 on planar c-Si without annealing illustrates a high reflection in the short wavelength region (350-800 nm). The reflection is 18.5% at a wavelength of 600 nm. The AWR of this sample is 22.3%. The reflection of the Al_2O_3 annealed at 700 ºC falls to 13.3% at a wavelength of 600 nm (with AWR of 21.2%). This leads to absorption of around 86.7% at the same wavelength. With 800 ºC annealing, the reflection reduces to 8% at 600 nm with AWR of 21%. This is attributed to enhanced light-coupling by the Al_2O_3 ARC on the c-Si at the higher annealing temperature. This leads to absorption of 92% at a wavelength of 600 nm.

https://scilett-fsg.uitm.edu.my/
Vol. 17(1) JANUARY 2023

ISSN: 1675-7785
eISSN: 2682-8626

DOI: 10.24191/sl.v17i1.18897

From Figure 4 (b), it can be observed that there is a decrease of absorption above 800 nm wavelength when the annealing temperature is increased to 800 °C and 900 °C. When annealed at 900 °C, the reflection reduces to about 6% at 600 nm with an AWR of 20.4%. This is lower than 800 °C, and the light absorption increases to 94% at the same wavelength.

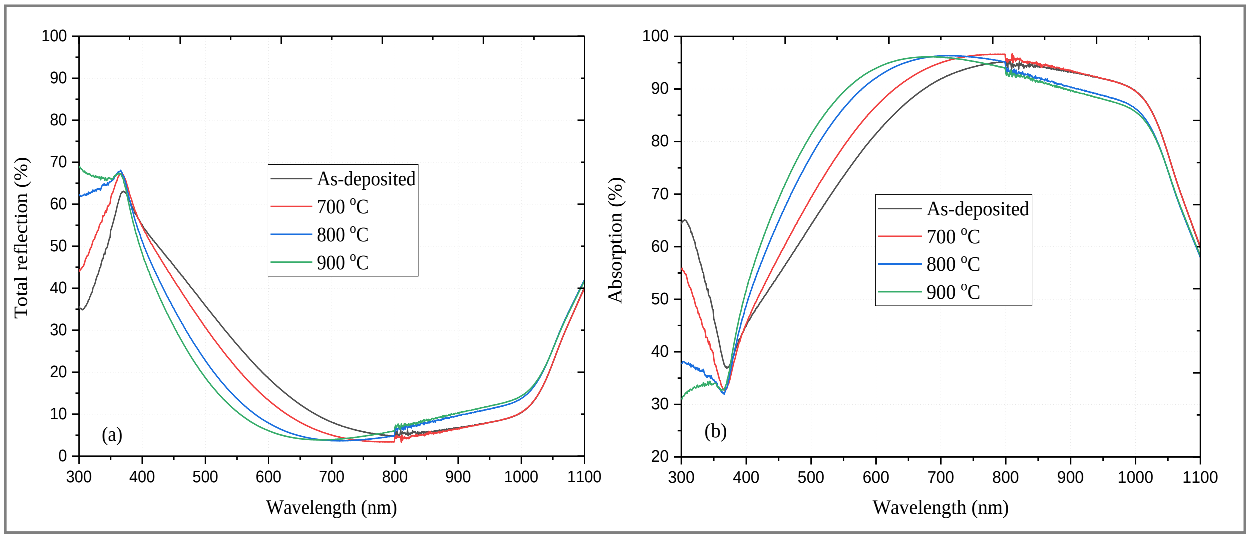

Figure 4: (a) Total reflection and (b) absorption curves of Al_2O_3 deposited on planar c-Si wafers, followed by annealing at different temperatures; 700 °C, 800 °C and 900 °C. Note that as-deposited (without annealing) Al_2O_3 on planar c-Si is included for comparison.

Table 1 demonstrates the summary of AWR and potential $J_{sc(max)}$ of Al_2O_3 ARC on c-Si without annealing and with different annealing temperatures from 700 °C to 900 °C, as calculated by Equation (2). Note that potential $J_{sc(max)}$ enhancement (%) is calculated by normalising the improved potential $J_{sc(max)}$ of the sample over the potential $J_{sc(max)}$ of the Al_2O_3 on planar c-Si reference without annealing. The Al_2O_3 on planar c-Si without annealing temperature has AWR of 22.3% and potential $J_{sc(max)}$ of 35.4 mA/cm^2.

When the Al_2O_3 on planar c-Si annealed at 700 °C, the AWR reduces to 21.2%, and the potential $J_{sc(max)}$ increases to 36.4 mA/cm^2 due to the lower light reflection in short wavelength (350-800 nm) region. This corresponds to a 2.8% enhancement compared to the Al_2O_3 without annealing and is attributed to the improved broadband light absorption by the Al_2O_3 roughness on the wafer surface. With 800 °C annealing, the potential $J_{sc(max)}$ increases to 36.9 mA/cm^2. This is a 4.2% enhancement when compared to the Al_2O_3 without annealing. Al_2O_3 ARC annealed at 900 °C demonstrates an increase of potential $J_{sc(max)}$ to 37.3 mA/cm^2 (or 5.4% enhancement) with AWR of 20.4% due to improved broadband light-coupling into the planar c-Si absorber. This is believed to be contributed by the highest RMS roughness (i.e. 10.7 nm) of the ARC layer on the c-Si wafer.

Table 1: Summary of AWR (within 300-1100 nm wavelength region), calculated potential $J_{sc(max)}$ and $J_{sc(max)}$ enhancement of Al_2O_3 on planar c-Si wafers with different annealing temperatures. The $J_{sc(max)}$

ISSN: 1675-7785
eISSN: 2682-8626

DOI: 10.24191/sl.v17i1.18897

enhancement (%) is calculated by normalising the improved potential $J_{sc(max)}$ of the Al_2O_3 on planar c-Si with annealing over the potential $J_{sc(max)}$ of the Al_2O_3 on planar c-Si without annealing (as-deposited)

Sample	**AWR (%)**	**Potential $J_{sc(max)}$ (mA/cm^2)**	**Potential $J_{sc(max)}$ enhancement (%)**
As-deposited	22.3	35.4	-
700 ^oC	21.2	36.4	2.8
800 ^oC	21.0	36.9	4.2
900 ^oC	20.4	37.3	5.4

CONCLUSION

In this work, the impact of annealing towards the anti-reflection properties of Al_2O_3 on planar mono c-Si wafers is investigated. The Al_2O_3 ARC with 120 nm thickness is deposited on the c-Si wafers by RF sputtering. This is followed by annealing at different temperatures (700-900 ^oC) for 20 min in N_2 ambient. From the AFM images, the surface of the Al_2O_3 on c-Si without annealing temperature is smooth, with an RMS surface roughness of 1.9 nm. The RMS roughness increases with increased annealing temperature. The RMS roughness for Al_2O_3 ARC on planar c-Si annealed at 700 ^oC, 800 ^oC and 900 ^oC demonstrates illustrates an increasing trend; 4.4 nm, 7.3 nm and 10.7 nm, respectively. The Al_2O_3 ARC on planar c-Si without annealing exhibits reflection of 18.5% at a wavelength of 600 nm, with AWR of 22.3% and potential $J_{sc(max)}$ of 35.4 mA/cm^2. With annealing at 700 ^oC, the reflection of the Al_2O_3 reduces to 13.3% at the same wavelength. This leads to AWR of 21.2% and absorption of around 86.7% at the same wavelength. With 800 ^oC annealing, the reflection reduces to 8% at 600 nm with AWR of 21%. After annealing at 900 ^oC, the reflection reduces to about 6% at 600 nm with an AWR of 20.4%. This is lower than the AWR of 800 ^oC annealing and results in the highest absorption enhancement from 400 to 700 nm wavelength with potential $J_{sc(max)}$ of 37.3 mA/cm^2 due to the increase in the RMS surface roughness of the Al_2O_3 ARC on the planar c-Si substrate.

ACKNOWLEDGMENTS

The authors would like to acknowledge Universiti Sains Malaysia (USM), Penang, for funding this research through Short-Term Grant 304/PFIZIK/6315063. The first author would like to acknowledge the Department of Physics, Faculty of Science and Health, Koya University.

https://scilett-fsg.uitm.edu.my/
Vol. 17(1) JANUARY 2023

ISSN: 1675-7785
eISSN: 2682-8626

DOI: 10.24191/sl.v17i1.18897

AUTHOR'S CONTRIBUTION

All the authors contributed to the study design, data analysis and writing of the manuscript.

CONFLICT OF INTEREST STATEMENT

The authors agree that this research was conducted without any self-benefits or commercial or financial conflicts and declare the absence of conflicting interests with the funders.

REFERENCES

[1] Pera, D. M., Costa, I., Serra, F., Gaspar, G., Lobato, K., Serra, J. M., & Silva, J. A. (2023). Development of a metal-assisted chemical etching method to improve light-capture in monocrystalline silicon solar cells. *Solar Energy Materials and Solar Cells*, *251*, 112143. doi.org/10.1016/j.solmat.2022.112143

[2] Lukhman, S., Natar, N., Ghani, N., Shukor, A., Nazeri, S., Ikhwan, S., Badri, A., Hamzah, R., Rosli, A., Razak, S., & Izhan, W. (2021). Preparation of Polyaniline/TiO_2 Photovoltaic Solar Cell. *Science Letters*, *15 (*2), 102-115. doi.org/10.24191/sl.v15i2.13833

[3] Wang, Q., Yao, P., Li, Y., Jiang, L., Xu, J., Liang, S., ... & Liu, H. (2023). Inverted pyramid structure on monocrystalline silicon processed by wet etching after femtosecond laser machining in air and deionized water. *Optics & Laser Technology*, *157*, 108647. doi.org/10.1016/j.optlastec.2022.108647

[4] Nauryzbekova, S., Nussupov, K., & Bakranova, D. (2022). Simulation of antireflective coatings system based on Porous Si/DLC and SiO_2/TiO_2 for Si solar cells. *Materials Today: Proceedings*, 49, 2474–2477. doi.org/10.1016/j.matpr.2020.11.673

[5] Payne, D., Fung, T.H., Khan, M.U., Cruz-Campa, J., McIntosh, K., & Abbott, M. (2018). Understanding the optics of industrial black silicon. *AIP Conference Proceedings*, 1999.

[6] Zhang, D., Wang, L., Jia, R., Tao, K., Jiang, S., Ge, H., ... & Jin, Z. (2022). Improving the performance of PERC silicon solar cells by optimizing the surface inverted pyramid structure on large-area mono-crystalline silicon wafers. *Materials Science in Semiconductor Processing*, *138*, 106281. doi.org/10.1016/j.mssp.2021.106281

[7] Omar, H.D., Hashim, M.R., & Pakhuruddin, M.Z. (2020). Ray tracing of inverted pyramids for light-trapping in thin crystalline silicon for solar cells. *Optik*, 219, 165279.

[8] Zhang, J., Zhang, S., Jiang, X., Yao, J., Wang, A., & Zhan, Q. (2023). Numerical study on flat dispersion in a single-layer Si3N4 coupled-waveguides with four zero-dispersion wavelengths for supercontinuum generation. *Optics & Laser Technology*, *160*, 109061. doi.org/10.1016/j.optlastec.2022.109061

[9] Zin, N., McIntosh, K., Bakhshi, S., Vázquez-Guardado, A., Kho, T., Fong, K., ... & Blakers, A. (2018). Polyimide for silicon solar cells with double-sided textured pyramids. *Solar energy materials and solar cells*, *183*, 200-204. doi.org/10.1016/j.solmat.2018.03.015

[10] Ahn, S., Hong, S. J., Yang, H. S., & Cho, S. M. (2022). Effect of 2 MHz frequency power applied

https://scilett-fsg.uitm.edu.my/
Vol. 17(1) JANUARY 2023

ISSN: 1675-7785
eISSN: 2682-8626

DOI: 10.24191/sl.v17i1.18897

to the substrate for low-temperature silicon nitride thin film deposition. *Materials Science in Semiconductor Processing*, *143*, 106538. doi.org/10.1016/j.mssp.2022.106538

[11] Shanmugam, N., Pugazhendhi, R., Madurai Elavarasan, R., Kasiviswanathan, P., & Das, N. (2020). Anti-reflective coating materials: a holistic review from PV perspective. *Energies*, *13*(10), 2631. 1; doi.org/10.3390/en13102631

[12] Schmidt, J., Werner, F., Veith, B., Zielke, D., Steingrube, S., Altermatt, P. P., ... & Brendel, R. (2012). Advances in the surface passivation of silicon solar cells. *Energy Procedia*, *15*, 30-39. doi.org/10.1016/j.egypro.2012.02.004

[13] Singh, P., Jha, R. K., Singh, R. K., & Singh, B. R. (2018). Preparation and characterization of Al2O3 film deposited by RF sputtering and plasma enhanced atomic layer deposition. *Journal of Vacuum Science & Technology B, Nanotechnology and Microelectronics: Materials, Processing, Measurement, and Phenomena*, *36*(4), 04G101. doi.org/10.1116/1.5023591

[14] Angarita, G., Palacio, C., Trujillo, M., & Arroyave, M. (2017, June). Synthesis of alumina thin films using reactive magnetron sputtering method. In *Journal of Physics: Conference Series* (Vol. 850, No. 1, p. 012022). IOP Publishing. doi.org/10.1088/1742-6596/850/1/012022

[15] Zhao, Y., Zhou, C., Zhang, X., Zhang, P., Dou, Y., Wang, W., ... & Zhou, S. (2013). Passivation mechanism of thermal atomic layer-deposited Al 2 O 3 films on silicon at different annealing temperatures. *Nanoscale Research Letters*, *8*(1), 1-7. doi.org/10.1186/1556-276X-8-114

[16] Kern, W. (1990). The evolution of silicon wafer cleaning technology. *Journal of the electrochemical society*, 137, 1887.

[17] Omar, H. D., Hashim, M. R., & Pakhuruddin, M. Z. (2021). Optimization of etching time for enhanced broadband absorption in flexible black silicon on stainless steel foil. *Optik*, *225*, 165781. doi.org/10.1016/j.ijleo.2020.165781

[18] Zhao, F., Chen, X., Yi, Z., Qin, F., Tang, Y., Yao, W., ... & Yi, Y. (2020). Study on the solar energy absorption of hybrid solar cells with trapezoid-pyramidal structure based PEDOT: PSS/c-Ge. *Solar Energy*, *204*, 635-643. doi.org/10.1016/j.solener.2020.05.030

[19] Pakhuruddin, M. Z., Huang, J., Dore, J., & Varlamov, S. (2015). Light absorption enhancement in laser-crystallized silicon thin films on textured glass. *IEEE Journal of Photovoltaics*, *6*(1), 159-165. doi.org/10.1109/JPHOTOV.2015.2501727

[20] Wang, Z. Y., Zhang, R. J., Lu, H. L., Chen, X., Sun, Y., Zhang, Y., ... & Chen, L. Y. (2015). The impact of thickness and thermal annealing on refractive index for aluminum oxide thin films deposited by atomic layer deposition. *Nanoscale research letters*, *10*(1), 1-6. doi.org/10.1186/s11671-015-0757-y